

## Macro Model Simulating the Seismic Force Resisting Mechanism of Multi-Story Shearwalls Supported by Piles

Masanobu Sakashita<sup>1</sup>, Fumio Watanabe<sup>2</sup>, Susumu Kono<sup>3</sup> and Hitoshi Tanaka<sup>4</sup>

<sup>1</sup> Assistant Professor, Dept. of Architecture and Architectural Engineering, Kyoto University, Japan.

<sup>2</sup> Professor Emeritus, Dept. of Architecture and Architectural Engineering, Kyoto University, Japan

<sup>3</sup> Associate Professor, Dept. of Architecture and Architectural Engineering, Kyoto University, Japan

<sup>4</sup> Professor, Disaster Prevention Research Institute, Kyoto University, Japan

Email: sakashita@archi.kyoto-u.ac.jp, kono@archi.kyoto-u.ac.jp

### ABSTRACT :

Structural walls are supported by foundation beams and piles that transfer earthquake-induced forces from the structural walls to the soil. In the current design procedure, the structural walls are normally assumed to stand on the solid foundation. This assumption makes it possible to evaluate the seismic behavior of each member independently. However, in case that the foundation beams don't have enough strength and stiffness to resist against seismic lateral forces, unexpected lateral load resisting mechanism can be formed. The resulting stress state may be completely different from that based on the assumption of the solid foundation. This study aims to analytically clarify the lateral load resisting mechanism of the structural wall system considering the interaction between the structural wall, the foundation beam and the piles. In order to make clear the interaction, one 25% scale specimen was modeled in two different ways. Difference of the models was with or without the pile foundation of the specimen. A pushover analysis with these models was performed. The analytical models made clear the differences of the lateral load resisting mechanism. Experimental results, such as hysteretic curve of the structural wall, deformation and damage, could be simulated well by the model with the pile foundation. It was confirmed that the upper longitudinal bars in the foundation beam played an important role in the formation of the rotational mechanism of the wall pile assemblage that were observed in experiment and analysis.

**KEYWORDS:** Structural wall, Foundation beam, Pile, Macro model, Interaction

### 1. INTRODUCTION

Typical Japanese RC mid-rise and high-rise residential buildings have multiple bay moment resisting frames in the longitudinal direction and single bay structural wall systems in the transverse direction. The structural walls are widely used for buildings in order to provide high stiffness and strength against seismic lateral forces. The structural walls are also supported by foundation beams and piles that transfer earthquake-induced forces from the structural walls to the soil. In current design procedures, the structural walls are normally assumed to stand on solid foundation. This assumption makes it possible to evaluate the seismic behavior of each member independently. As extensive studies have been conducted based on this assumption, design procedures for these structural members are well established. However, whether the assumption is valid or not is hardly confirmed.

The structural wall and the foundation beam are cast monolithically. If the foundation beam doesn't have sufficient stiffness and strength, there is a possibility that they can resist against seismic lateral forces like one structural wall whose base is supported by piles. In this case, the resulting stress state may be completely different from that based on the assumption of solid foundation.

It is commonly known that the flexural behavior of the structural walls has influence on the lateral load resisting mechanism of the walls. Shear transfer mechanism at the wall bases varies according to the deformation levels of the walls. Hirose et al. actually monitored shear forces acting on the wall base with load cells, and clarified the transition of the shear transfer mechanism [5]. Most of these studies were conducted assuming that the foundation beams should be infinitely rigid. However, in our earlier experimental study where the structural wall with pile foundation was tested [6], it was confirmed that the assumption of solid foundation beam wasn't always valid. Thus in order to establish the rational design procedures, it is necessary

to clarify the interaction between the structural walls, the foundation beams and piles.

This study aims to analytically clarify the lateral load resisting mechanisms considering the interaction between the structural wall, the foundation beam, the slabs and the piles. The analytical object was one 25% model specimen. Details of the experiment using this specimen have been already reported [6]. The specimen was modeled in two different ways. Difference of the models was with or without the pile foundation of the specimen. A pushover analysis with these models was performed. From comparison between the experimental results and the analytical results, the adequacy of the proposed model was confirmed and the lateral load resisting mechanism of the structural wall-pile foundation assemblage was clarified.

## 2. EXPERIMENTAL STUDY

### 2.1. Specimen and test setup

Figure 1 shows specimen configuration and Table 1 shows types of reinforcement. The specimen configuration was determined from typical fourteen story residential buildings in Japan. They normally have multiple spans of a moment resisting frame in the longitudinal direction and a single span of structural wall system in the transverse direction. The assemblage consisted of the lowest three floors of structural wall with a foundation beam, the first floor slab, and two piles. In this study, the structural wall was designed to fail in flexure and develop a single plastic hinge at the base. The flexural behavior of the structural wall could have influence on the transition of shear transfer mechanism at the wall base. The piles were designed to be elastic during the loading test in order to concentrate deformation on the wall base. Figure 2 shows loading system in this experiment. Lateral load  $Q$  was applied statically through a 1000kN horizontal jack (A) to the center of the loading beam. Two 2000kN vertical jacks were adjusted to create appropriate column axial forces at the structural wall base,  $N_1$  and  $N_2$ , which are a liner function of lateral load  $Q$  to simulate loading conditions of the prototype fourteen-story structural wall system under earthquakes.

$$N_1 \text{ and } N_2 = \pm 2.27Q + 353 \text{ (unit:kN)} \quad (1)$$

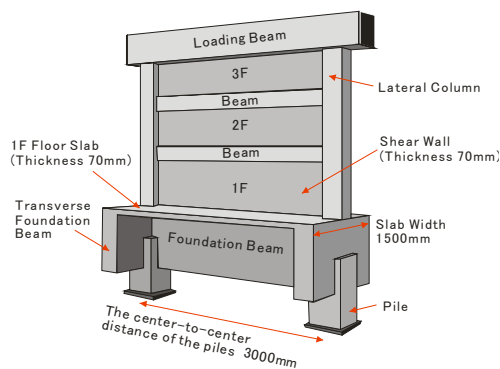


Figure 1 Specimen configuration

Table 1 Types of reinforcement

Member (unit:mm)	Type of bars			Steel Ratio (%)
Column (260 × 260)	Longitudinal	8-D13	SD295A	1.50
	Transverse	2-D10@100	KSS785	0.549
Beam (140 × 200)	Longitudinal	4-D10	SD295A	1.18
	Transverse	2-D6@150	SD295A	0.302
Shear Wall (Thickness 70mm)	Vertical	D6@150	SD295A	0.302
	Horizontal	D6@150	SD295A	0.302
Foundation Beam (150 × 880)	Longitudinal	4-D22	SD295A	1.26
	Transverse	2-D10@150	SD295A	0.634
Slab (Thickness 70mm)	Longitudinal	D6@150	SD295A	0.302
	Transverse	2-D13@120	SD295A	0.480

Table 2 Material properties of concrete and reinforcement

(a) Concrete

	Compressive strength (MPa)	Tensile strength (MPa)	Young's modulus (GPa)
Foundation beam, Pile	45.7	3.41	25.9
Wall, Column, Beam	60.3	3.32	30.4

(b) Reinforcement

	Yield strength (MPa)	Tensile strength (MPa)	Young's modulus (GPa)
D6	377	532	179
D10(SD295A)	378	511	183
D10(KSS785)	919	1078	201
D13	351	505	175
D16	337	502	191
D22	341	525	183
D32	387	585	188

Piles were supported by pin and roller respectively. At the roller support,  $0.7Q$  was applied horizontally to the pile on the compressive side and  $0.3Q$  was applied to the pile on the tensile side by a 1000kN jack (B) in the

opposite direction to the 1000kN horizontal jack (A). The lateral load applied to the pile induces moment from piles shown in Figure 3. In Japanese design guideline, the amount of the longitudinal reinforcement in foundation beams is determined by the moment from piles and half of the lateral load  $Q/2$ . The deformation of the specimen was evaluated using that of the first story structural wall. The first story drift angle, which is hereinafter called  $R$ , was calculated from the flexural deformation and shear deformation. The displacement control was used with two cycles at each prescribed displacement.

## 2.2. Experimental results

Figure 4 shows crack distribution at  $R=0.8\%$ . Flexural cracks took place at tensile columns and propagated to flexural shear cracks in the wall panels. These cracks penetrated the slabs transversely and extended to the foundation beam. As the deformation of the structural wall propagated, these cracks in the foundation beam became dominant and opened up near the compressive columns, which was circled by dotted line in Figure 4.

Figure 5 shows the deformation mechanism of the specimen that is assumed from the experimental results. As these cracks in the foundation beam opened up, the wall and the right pile together with the right top corner of the foundation beam made a solid assemblage rotated almost rigidly about Point P. Thus the assumption of infinitely rigid foundation beam wasn't valid in this experiment. The upper longitudinal bars in the foundation beam are arranged to prevent these cracks from opening up as shown in Figure 5, so they are assumed to play an important role in the formation of the rotational mechanism of the wall pile assemblage.

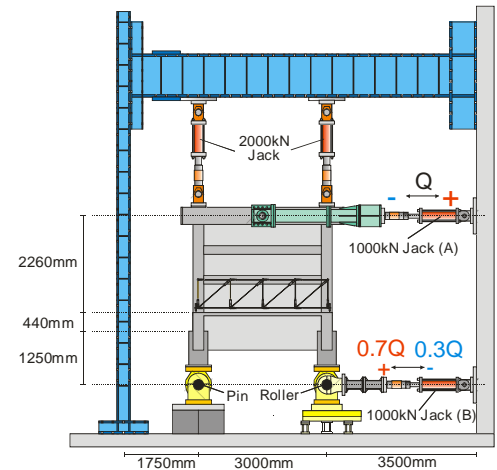


Figure 2 Loading system

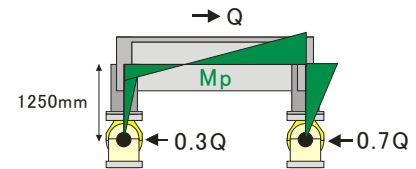


Figure 3 Moment from piles

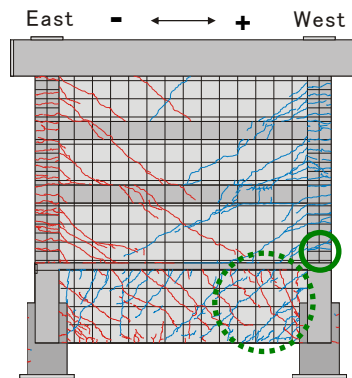


Figure 4 Crack distribution ( $R=0.8\%$ )

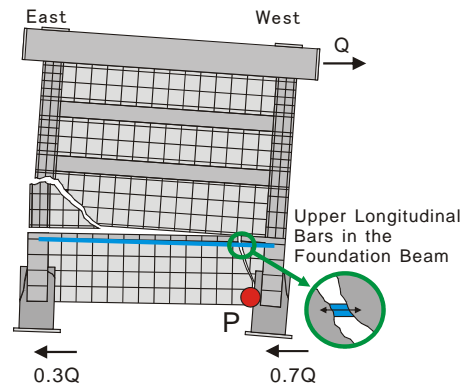


Figure 5 Deformation mechanism

Figure 7 shows lateral load-the first story drift angle relationship in positive direction. After yielding of the longitudinal bars in the tensile columns, lateral load applied to the loading beam continued to increase gradually and it showed high ductility. Compressive failure of concrete at the compressive column bases is often observed when the structural walls that fail in flexure are tested. As the flexural deformation at the wall bases propagates, compressive area of concrete at the column bases decreases. It causes the rapidly decreasing of the resistance to the lateral load. In this experiment, the structural wall was loaded monolithically to  $+4.1\%$ . However, compressive failure of the cover concrete at the column bases was hardly observed, which was circled by solid line in Figure 4. The high ductility was thought to be due to the rotational behavior of the wall pile assemblage. Unlike the flexural behavior, the rotational behavior doesn't decrease the compressive area at the column bases.

### 3. ANALYTICAL STUDY

#### 3.1. Analytical model

Various analytical models have been proposed for predicting the inelastic response of structural walls [8]. Figure 7 shows TVLEM (three vertical line element model). TVLEM is one of these analytical models. They have some vertical line elements that represent restoring force characteristic of each deformation. They are used widely, because it is easy to install the frame analysis. Commonly they have infinitely rigid beams at the top and bottom levels. It is known that these beams are restricted by the upper and lower wall panels and their flexural and shear deformations can be negligible. In addition, considering the local stress transfer through vertical line elements, the beams should be modeled as infinitely rigid elements.

However, from the experimental study, it was clarified that the assumption of infinitely rigid foundation beam wasn't always valid. As the rotation of the wall pile assemblage was observed in experiment, the behaviors of the structural wall and the pile foundation system should be considered at the same time. The specimen was modeled as shown in Figure 8(a). This model is hereinafter called Specimen Model. In addition to Specimen Model, Wall model was introduced to make clear the behavior of the structural wall itself. The structural wall of Specimen Model was the same as Wall Model. From comparison between Specimen Model and Wall Model, the interaction can be clarified. The boundary condition and the load condition of the models were basically the same as those in experiment. The nodes in the wall base of Wall Model were fixed by pin supports.

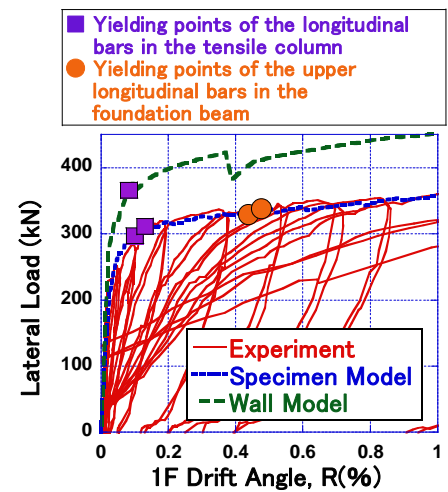


Figure 6 Lateral load - the first story drift angle relationship

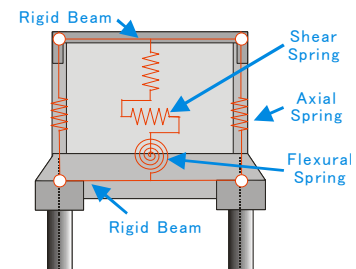


Figure 7 TVLEM

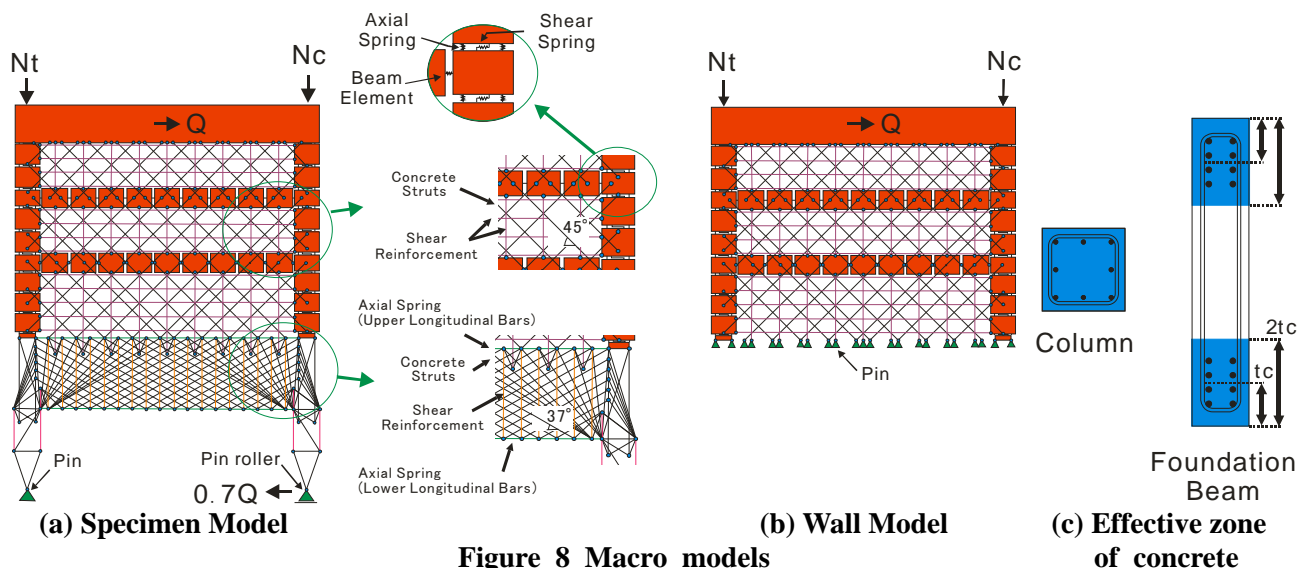


Figure 8 Macro models

They were modeled as assembly of rigid elements, truss elements and beam elements. The truss elements could be divided into four types of elements, axial spring, shear spring, shear reinforcement and concrete strut. Longitudinal bars in the columns, the foundation beam and the piles were modeled as the axial springs. In order to enhance the accuracy of the analysis, the tension-stiffening model was introduced to the axial springs. It represents the bond effect between concrete and longitudinal reinforcement. Beam elements were used to

simulate the behavior of the beams in the structural wall. As noted above, the beams in the structural walls are normally expressed as infinity rigid elements in various analytical models. In this study, sufficient flexural and shear stiffness were given to the beam elements and only the axial deformation was permitted. The tension-stiffening model wasn't introduced to the beam elements. In modeling the axial springs and the beam elements, it is necessary to determine the effective zones of concrete that contribute to the axial stiffness and strength of each model. The effective zones were determined as shown in Figure 8(c). The effective zones of the members without concrete struts, such as the columns and the beams, were determined to be the total cross sections. The effective zones of the members with concrete struts, which were the foundation beam and the piles, were decided as follow. The thickness of the effective zones was assumed to be twice as much as the distance from the center of the longitudinal bars to the surfaces of the members.

**Table 4 Structural elements introduced to each member**

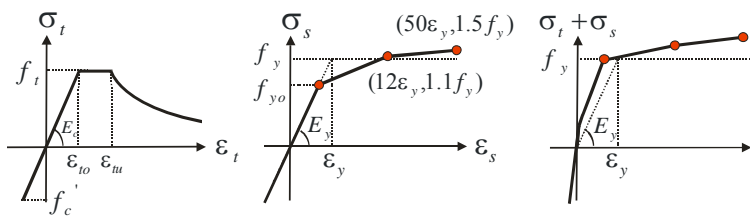
	Rigid element	Truss element				Beam element
		Axial spring	Shear spring	Shear reinforcement	Concrete struts	
Loading beam	●					
Column	●	●	●			
Beam	●					●
Wall panel					●	
Foundation beam		●			●	
Pile		●			●	

The structural wall was modeled based on Takehara et al. study [9]. It consisted of the columns, the beams and the wall panels. The columns were modeled by the rigid elements, the axial springs and the shear springs. The axial springs were placed at the center of the main reinforcement of one side row. The concrete struts and the shear reinforcement in the wall panels were fasten to the surrounding frame. The concrete struts were arranged assuming that the diagonal cracks have been formed and significantly developed in the wall panels. The angle of the inclined concrete struts  $\theta$  was assumed to be 45 degree in this study.

The foundation beam and piles were modeled by the axial springs, the concrete struts and the shear reinforcement. The lengths of the axial springs in the foundation beam were determined by the spacing of the shear reinforcement, which also decided the thickness of the concrete struts in the structural wall and the foundation beam. The angle of the inclined concrete struts of the foundation beam was assumed to be 37 degree based on the results of the parametric study.

Figure 9 shows the tension-stiffening model proposed by Maekawa et al. [10, 11]. The stress-strain relationship of concrete in tension is shown in Figure 9 (a). The tensile limit strain  $\varepsilon_{tu}$  is twice as much as the tensile strain  $\varepsilon_{to}$  for tensile strength  $f_t$  of the concrete. After a crack takes place, tensile stress is determined by Equation (2). The stress-strain relationship of longitudinal reinforcement is expressed by a tri-linear model as shown in Figure 9(b). The steel strain and the steel strength are given as average values, so the tensile stress at yielding point is lower than its yield strength.

$$\sigma_t = f_t (\varepsilon_{tu} / \varepsilon_t)^{0.4} \quad (2)$$

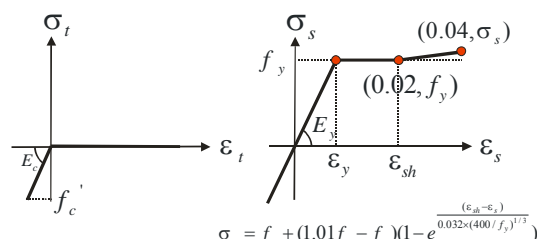


(a) Concrete

(b) Steel

(c) a + b

**Figure 9 Tension-stiffening model**



(a) Concrete

(b) Steel

**Figure 10 Models for materials**

The stress-strain relations of the other elements without considering the tension-stiffening effect, such as concrete struts, shear reinforcement and beam elements, are shown in Figure 10. In this study, compressive stress level acting on concrete struts was relatively low, so the stress-strain relation of concrete in compression was expressed by elastic model. Concrete tensile stress wasn't considered. Those of shear reinforcement were represented by a tri-linear model, as shown in Figure 10(b). The stress-strain relations of the axial springs in compression were also expressed by the same models shown in Figure 10.

Takehara et al. [9] proposed the stiffness of the shear springs in the columns,  ${}_cK_{ns}$  as follow.

$${}_cK_s = GbD {}_cK_n / (\Delta h \cdot K_{nc}) \quad (3)$$

$${}_cK_{nt} = E_s A_g / (2\Delta h) \quad (4)$$

$${}_cK_{nc} = (E_s A_g + E_c bD) / (2\Delta h) \quad (5)$$

where  ${}_cK_n$  is an average stiffness of two axial springs shown in Figure 8(a) at the same loading cycles. The term of  ${}_cK_n / {}_cK_{nc}$  in Equation (3) expresses the reduction of the shear rigidity due to the progress of horizontal cracks.  ${}_cK_{nt}$  and  ${}_cK_{nc}$  are the stiffness of the axial springs in tension and in compression respectively. For the sake of simplification, in this study, the stiffness of the shear springs was expressed as constant number. The shear stiffness of tensile column and that of compressive column were determined assuming that  ${}_cK_n$  was equal to  ${}_cK_{nt}$  and  ${}_cK_{nc}$  respectively.  $G$  is concrete shear modulus.  $b$  and  $D$  is the width and depth of the columns respectively.  $\Delta h$  indicates the heights of the rigid elements.  $E_c$  and  $E_s$  are Young's modules of concrete and reinforcement.  $A_g$  is the area of the longitudinal bars in the column.

### 3.2. Analytical results

Figure 6 and Table 3 show the comparison between experimental results and analytical results. As shown in Figure 6, Wall Model overestimated the strength and the stiffness of the envelope curve in experiment. On the other hand, the envelope curve of Specimen Model agreed well with that of experiment. Specimen Model also predicted the yielding points of the longitudinal bars in the tensile column and the upper longitudinal bars in the foundation beam. Table 3 shows the flexural deformation and shear deformation at representative loading stages. The loading stages of the analytical models were determined so as to correspond to the flexural deformation in experiment. In this experiment, the first story drift angle was calculated by summing the flexural deformation and shear deformation of the first story. Though Wall Model underestimated the amount of the shear deformation in experiment, Specimen Model predicted the amount of the shear deformation in experiment at each loading stage as well as the hysteretic curve. These results show that the interaction of the structural wall-foundation assemblage can't be neglected in order to predict the envelope curve of the structural wall. From here, the differences of the lateral load resisting mechanism between Specimen Model and Wall Model are assessed specifically.

**Table 3 Flexural deformation and shear deformation at representative loading stages**

	Loading stages	Flexural deformation (%)	Shear Deformation (%)	1F Drift Angle (%)	Lateral Load (kN)
Experiment	(a)	0.046	0.134	0.180	319.2
	(b)	0.136	0.397	0.533	341.4
	(c)	0.203	0.632	0.835	353.3
Specimen Model	(a)	0.046	0.122	0.169	310.8
	(b)	0.135	0.321	0.456	333.1
	(c)	0.202	0.461	0.663	339.6
Wall Model	(a)	0.044	0.061	0.105	367.5
	(b)	0.130	0.131	0.261	408.0
	(c)	0.204	0.203	0.407	389.9

Figure 11 shows deformations of each model. Figure 12 shows distributions of the compressive forces acting on concrete struts. The thickness of each concrete strut indicated the amount of the compressive force. The base of the Wall Model was fixed by pin supports assuming that it would stand on the solid foundation. From Table 3, it is clear that the ratio of the flexural deformation in Wall Model is larger than that in Specimen Model. As

shown in Figure 11(b), the compressive column base was deformed largely by flexure in Wall Model. Compressive resultant force by flexure and shear force transferred through the concrete struts concentrated on the compressive column base, which is circled by solid line in Figure 12(b). In this analysis, the flexural behavior of the columns was modeled only by two axial springs, so they were not enough to express the progress of the compressive failure of the cover and core concrete. The degradation of lateral load carrying capacity wasn't observed in this analysis, but there is a possibility that it leads to severe damage. Figure 11(a) shows the deformation of Specimen Model. The wall and the right pile together with the right top corner of the foundation beam made a solid assemblage rotated almost rigidly about Point P, which was almost the same as the assumed deformation mechanism shown in Figure 5. Unlike Wall Model, the deformation of the compressive column base was minimal. As shown in Figure 12(a), the compressive force and the shear force were transferred through relatively large area in the wall base even at large drift angle. It enabled the structural wall to have high ductility. These analytical results of Specimen Model corresponded to the experimental results.

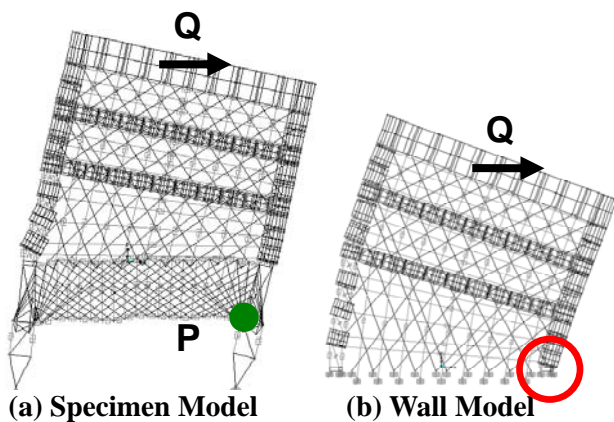


Figure 11 Deformations of macro models (R=1.0%)

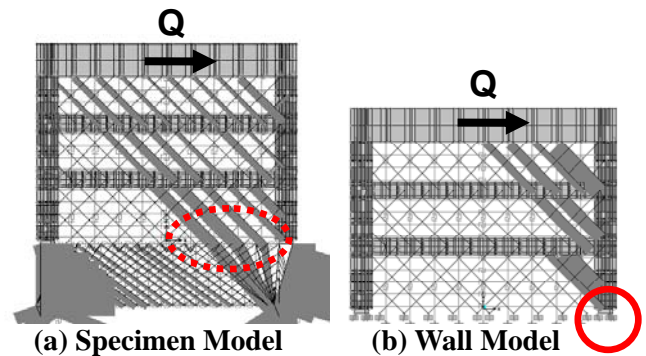


Figure 12 Distributions of the compressive forces acting on the concrete struts (R=1.0%)

Figure 13 shows the relationship between elongation of the upper longitudinal bars in the foundation beam and the first story drift angle of the structural wall. The elongation was calculated by integrating strain along the longitudinal reinforcement in the whole span of the foundation beam. The strain of the longitudinal bars in experiment was measured with multiple strain gauges. From experimental results, it is clear that the elongation is linearly proportional to the drift angle. And this relationship continues even after the lateral load reached the plateau. Specimen Model could also predict this linear relationship with good accuracy. These results verify the formation of the rotational mechanism of the wall pile assemblage shown in Figure 5. It also implies that the upper longitudinal bars should be designed considering the drift angle of the structural wall. Especially at large drift angle, the required stress or strain of the upper longitudinal bars can be underestimated if the conventional design procedures explained in chapter 2.1 is used. In order to avoid the formation of this rotational mechanism, it may be necessary to prevent flexural shear cracks from developing to the foundation beam or to arrange sufficient amount of the upper longitudinal bars in the foundation beam.

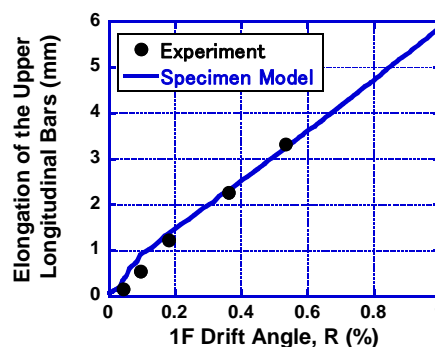


Figure 13 Elongation of the upper longitudinal bars-the first story drift angle, R relation

#### 4. CONCLUSIONS

In order to investigate the lateral load resisting mechanism of the structural wall-foundation assemblage, a pushover analysis was performed. One 25% scale specimen was modeled in two different ways. Difference of the models was with or without pile foundation of the specimen.

- The lateral load resisting mechanism of the Specimen Model was completely different from that of Wall Model. In the structural wall of Wall Model, the flexural deformation mode dominated the total deformation. Compressive resultant force by flexure and shear force were concentrated on the compressive column base. It may cause severe damage and lead to the degradation of lateral load carrying capacity. In Specimen Model, the rotation of the wall pile assemblage was confirmed. The envelope curve of the structural wall in Specimen Model showed lower stiffness and strength than that in Wall Model. However, due to the rotational behavior, ductility of the structural wall was improved. The analytical results of Specimen Model agreed with the experimental results.
- From the relationship between the elongation of the upper longitudinal bars in the foundation beam and the first story drift angle, the rotational behavior of the wall pile assemblage was verified. Their linear relationship implies that the upper longitudinal bars should be designed considering the drift angle of the structural wall. In order to avoid the formation of this rotational mechanism, it may be necessary to prevent flexural shear cracks from developing to the foundation beam or to arrange sufficient amount of the upper longitudinal bars in the foundation beam.

#### REFERENCES

- [1] Architecture Institute of Japan. (1999). *AIJ Standard for Structural Calculation of Reinforced Concrete Structures Based on Allowable Stress Concept*, 218-241. (In Japanese)
- [2] Paulay, T. Priestley, M.J.N. (1992). *Seismic Design of Reinforced Concrete and Masonry Buildings*. John Wiley & Sons, 362-499.
- [3] The building center of Japan. (1999). *Design and Construction Guidelines for Multiple Story Frame Structures with Shear Wall*, 9-54, 179-334. (In Japanese)
- [4] Architecture Institute of Japan. (2001). *Design Guidelines for Earthquake Resistant Reinforced Concrete Buildings Based on Inelastic Displacement Concept*, 191-240, 278-293, 320-327. (In Japanese)
- [5] Hirose T., Sanada Y., Yorkinov B. (2008). Detection of a weak point of a flexural wall by measuring shear transfer on its critical section. *Proceedings of the Japan Concrete Institute* **30:3**, 457-462. (In Japanese)
- [6] Sakashita M., Kono S., Watanabe F., Tanaka H. (2006). Lateral Force Resisting Mechanism of a Multi-story Shear Wall and Peripheral Members. *Proceeding of the 2nd fib Congress*, ID 9-17.
- [7] Sakashita M., Kono S., Watanabe F., Tanaka H. (2008). Deformation mechanism of flexural yielding multi-story shearwall supported on pile foundation. *Proceedings of the Japan Concrete Institute* **30:3**, 451-456. (In Japanese)
- [8] Kutay Orakcal, Leonardo M. Massone, John W. Wallace (2006). *Analytical Modeling of Reinforced Concrete Walls for Predicting Flexural and Coupled - Shear - Flexural Responses*, 7-20.
- [9] Takehara M., Mochizuki M., Onozato N., Akatsuka T. (1993), Elasto-plastic Analysis of Framed Shear Walls with an Opening Using Macro Model. *Summaries of Technical Papers of Annual Meeting Architectural Institute of Japan, Structures IV*, 303-304. (In Japanese)
- [10] Maekawa K., Fukuura N. (1999), Re-Formulation of Spatially Averaged RC Constitutive Model with Quasi-orthogonal Bi-directional Cracking, *Journals of the Japan Society of Civil Engineers* **No.634/V-45**, 157-176. (in Japanese)
- [11] Okamura H., Maekawa K. (1991), *Nonlinear Analysis and Constitutive Models of Reinforced Concrete*, Gihoudo-Shuppan
- [12] Miki T., Lertsamattiyakul M., and Niwa J., (2002), Numerical Evaluation for Flexural Deformation of Reinforced Concrete Columns Subjected to Axial and Flexural Loads Using Lattice Model, *Transactions of the Japan Concrete Institute* 2001, **Vol.23**, 231-238.